Civil and Environmental Engineering
Vol. 0, Issue 0, DOI: 10.2478/cee-2026-0111

Integrated Static–dynamic Assessment and Field-validated External Prestressing Strengthening of an Aging Steel Railway Bridge

Sumargo SUMARGO[1,*], Mardiana OESMAN[2], Fachmi FADLI[3]

[1] Department of Civil Engineering, Universitas Jenderal Achmad Yani, Cimahi, Indonesia.

[2] Department of Civil Engineering, Politeknik Negeri Bandung, Indonesia.

[3] Department of Civil Engineering, Politeknik TEDC Bandung, Indonesia.

* corresponding author: sumargo@lecture.unjani.ac.id

Date of Submission: 04 March 2026
Revision Date: 31 March 2026
Date of Acceptance: 31 March 2026

Civil and Environmental Engineering
Journal of the Faculty of Civil Engineering | University of Žilina

Abstract

The BH 25 steel truss railway bridge in Garut, Indonesia, exhibited a deviation from its intended camber during construction, raising concerns regarding its structural performance. This study presents an integrated assessment combining full-scale static and dynamic load testing with calibrated finite element modelling. A 90-ton CC206 locomotive was used to evaluate deflection and dynamic response. While the bridge satisfies serviceability requirements, a reduction in global stiffness is identified from its vibration characteristics. To mitigate this issue, an external prestressing system was implemented as a strengthening measure. The results confirm that the proposed intervention effectively restores camber and enhances dynamic performance. The study highlights the value of integrating field measurements with validated numerical modelling within a unified framework for both assessment and strengthening evaluation. This approach provides a practical basis for performance-based rehabilitation of steel railway bridges under operational conditions.

Keywords

Static load testing; Dynamic testing; Steel truss railway bridge; External prestressing; Structural strengthening.

1. Introduction

Load testing constitutes a fundamental component of railway bridge assessment, as it enables direct observation of structural response under actual service loading (Chacon, R., et al. 2024; Lantsoght, et al., 2024). Static and dynamic load tests remain indispensable for verifying safety, serviceability, and long-term structural performance, particularly for aging steel bridges subjected to material degradation and geometric imperfection (Cao, J., and An, L., 2023; Toporova, I., 2023).

This study is directed toward a comprehensive evaluation of the BH 25 steel truss railway bridge by integrating static and dynamic field testing with calibrated numerical modelling and strengthening assessment. The research focuses on quantifying serviceability performance, identifying stiffness degradation through measured dynamic characteristics, and

evaluating structural capacity under current railway loading demands. In addition, the study examines the effectiveness of external prestressing combined with local plate reinforcement as a strengthening strategy for aging railway bridges.

Rather than formulating isolated research questions, this study adopts a performance-oriented perspective in which static deflection behaviour, dynamic vibration response, and member-level capacity are jointly interpreted to characterize the structural condition of an aging bridge system and to justify strengthening intervention. Regulatory provisions on railway bridge safety and load testing establish the governing acceptance criteria and performance thresholds adopted in this study, as stipulated in the Regulation of the Minister of Transportation of the Republic of Indonesia No. 69 of 2018 (Regulation of the Minister of Transportation of the Republic of Indonesia, 2018).

Innocenzi et al. (2022) demonstrated the combined use of static and dynamic testing together with finite element modelling for evaluating bridge performance during proof load testing, primarily focusing on validation of structural behaviour and testing procedures. Similarly, Bayraktar et al. (2017) conducted comprehensive static and dynamic field testing of a long-span cable-stayed bridge, emphasizing the identification of dynamic characteristics and validation of analytical models under operational conditions. While these studies successfully combine experimental and numerical approaches for structural assessment, they mainly focus on model validation and structural performance evaluation. In contrast, the present study extends this framework by explicitly linking field-measured static and dynamic responses to post-strengthening performance and member-level capacity verification. In particular, the effectiveness of external prestressing is quantified through changes in camber, natural frequencies, and demand-to-capacity ratios, providing a direct connection between measured structural behaviour and strengthening decision-making. This distinction has been clarified in the revised manuscript to emphasize that the contribution of this study lies not merely in combining testing and modelling techniques, but in establishing a field-validated, performance-based assessment and strengthening evaluation workflow for aging railway bridges under operational loading conditions.

The novelty of this research lies in its integrated use of full-scale static and dynamic load testing as a unified basis for both structural diagnosis and strengthening evaluation. Unlike previous studies that treat load testing, numerical modelling, and strengthening analysis as separate tasks, this study explicitly calibrates a three-dimensional finite element model using field-measured static and dynamic responses and employs the calibrated model to quantitatively assess the effectiveness of external prestressing. By linking changes in vibration characteristics and camber restoration directly to post-strengthening capacity improvement, this study provides empirical evidence on stiffness enhancement mechanisms in aging steel railway bridges.

To address the above research gap, this study employs an integrated methodology that combines full-scale static and dynamic load testing with calibrated three-dimensional finite element modelling. The proposed framework enables simultaneous evaluation of serviceability performance, stiffness degradation, and member-level structural capacity, and provides a rational basis for assessing the effectiveness of external prestressing as a strengthening intervention. The detailed methodology adopted to achieve these objectives is presented in Section 3.

Unlike conventional bridge load testing studies that focus solely on serviceability verification, this research adopts a capacity-oriented perspective in which static deflection behaviour, dynamic stiffness indicators, and member-level demand-to-capacity ratios are jointly interpreted within a unified framework. This approach reduces epistemic uncertainty in structural diagnosis and enables strengthening decisions to be supported by field-validated quantitative evidence rather than code-based assumptions alone.

Bridges play a critical role in transportation networks, and their failure or degradation can significantly disrupt traffic operations. Hlinka et al. (2024) emphasized the importance of advanced analytical methods and numerical modelling in evaluating structural stability and load-carrying capacity, particularly in situations where bridge performance must be assessed under constrained conditions. Their work highlights the necessity of reliable analytical approaches to support decision-making in bridge management and rehabilitation.

Research Contributions

This study makes the following contributions to the assessment and strengthening of existing railway bridges:

(1) It proposes an integrated, full-scale assessment framework combining static load testing, dynamic vibration testing, and calibrated three-dimensional finite element modelling for aging steel railway bridges.

(2) It provides empirical field evidence quantifying stiffness degradation and recovery through changes in natural frequencies, camber restoration, and member-level capacity ratios before and after external prestressing.

(3) It demonstrates the effectiveness of external prestressing as a performance-based strengthening strategy by explicitly linking measured static and dynamic responses to post-strengthening structural capacity improvement.

2. Literature Review

Recent studies have highlighted the importance of integrating diagnostic surveys, load testing, and long-term monitoring to evaluate the structural performance of aging bridge systems. For instance, Borzovič et al. (2025) demonstrated that combining detailed inspections with field measurements provides a reliable basis for assessing the condition and residual capacity of deteriorated prestressed concrete bridges. Their findings emphasize that continuous monitoring and field-based evaluation are essential for maintaining operational safety when structural degradation is present.

Performance-based assessment supported by field measurements has become a dominant paradigm in railway bridge evaluation, particularly for aging steel structures subjected to cumulative deterioration and construction imperfections (Gedam et al., 2020; Chacón et al., 2024; Lantsoght et al., 2024). Static load testing remains the primary method for serviceability verification through deflection control, whereas dynamic testing provides complementary insight into stiffness degradation via changes in natural frequencies and mode shapes (Kim et al., 2022; Bertolesi et al., 2021; Nhung et al., 2023; Cao & An, 2023; Topurova, 2023). However, several studies have emphasized that satisfactory serviceability performance does not necessarily ensure adequate structural capacity, particularly for aging truss systems affected by material degradation and geometric imperfections (Bacinskas et al., 2013; Qi et al., 2011; Duvnjak et al., 2019). The evaluation of load-carrying capacity remains a critical aspect in the assessment of existing railway bridges. Odrobiňák et al. (2025) proposed an analytical approach combining finite element modelling with advanced stress-based verification methods to assess the structural capacity of railway bridge components. Their study demonstrates that integrating global structural analysis with detailed member-level verification provides a more comprehensive understanding of structural performance under railway loading conditions.

To address these limitations, strengthening strategies such as external prestressing and local plate reinforcement have been proposed to enhance stiffness and load-carrying performance (Recupero et al., 2014; Lou et al., 2021; Karavasilis et al., 2021; Atta et al., 2024; Zhao et al., 2025). External prestressing is especially attractive because it enables camber restoration and internal force redistribution without major alteration of the structural system. Nevertheless, most available investigations focus on analytical simulations or laboratory-scale experiments, with comparatively limited full-scale field validation under operational railway loading (Ren et al., 2025; Fang et al., 2024; Guo et al., 2024).

In parallel, bridge assessment research has increasingly shifted toward integrated workflows combining load testing, vibration monitoring, and numerical model calibration to reduce epistemic uncertainty in structural diagnosis (Bien et al., 2020; Duvnjak et al., 2020; Hekic et al., 2024; He et al., 2023; Zhou et al., 2025). Advances in wireless sensing, non-contact measurement systems, and data-driven structural health monitoring have further enhanced the feasibility of vibration-based assessment under operational conditions (Li & Ohkubo, 2024; Qiao et al., 2025; Fawad et al., 2023; Rahman et al., 2024; Zou et al., 2024).

Despite these developments, existing studies often treat load testing, model calibration, and strengthening evaluation as sequential or loosely connected tasks rather than components of a unified, field-validated performance framework. Moreover, quantitative evidence explicitly correlating changes in vibration characteristics with measurable improvements in member-level demand-to-capacity ratios remains scarce. This gap motivates the integrated static–dynamic assessment and strengthening evaluation framework adopted in the present study.

Comprehensive diagnostic surveys are essential for understanding the condition and performance of aging bridge infrastructure. Rehacek et al. (2025) demonstrated that combining visual inspection, material testing, and structural assessment techniques enables a more accurate evaluation of bridge deterioration and load-carrying capacity. Such integrated diagnostic approaches are particularly important for aging prestressed structures subjected to long-term environmental and operational effects.

Research Gap and Contribution

Despite extensive research on static load testing, dynamic identification, numerical modelling and strengthening techniques for railway bridges, these components are frequently addressed as independent or sequential procedures. Comprehensive full-scale investigations that explicitly integrate static and dynamic field measurements with calibrated three-dimensional finite element modelling to support capacity-oriented decision-making remain limited. In particular, empirical evidence directly correlating changes in vibration characteristics and camber restoration with quantified improvements in member-level demand-to-capacity ratios is scarce.

The present study addresses this gap by implementing an integrated static–dynamic assessment framework in which field-measured responses are used to calibrate a numerical model and to quantitatively evaluate the effectiveness of external prestressing strengthening. By linking stiffness indicators, camber recovery, and structural capacity verification within a unified workflow, this research provides field-validated evidence supporting performance-based strengthening strategies for aging steel railway bridges.

3. Methodology

3.1. Bridge Description

The BH 25 railway bridge is located in Garut, West Java Province, Indonesia, and serves as part of an active railway corridor. It is a three-span steel truss bridge with a total length of 41.055 m, consisting of spans of span 1: 9.485 m, span 2: 21.930 m, and span 3: 9.635 m. Spans 1 and 3 consist of steel girder-type systems, in which the main load-bearing elements are longitudinal girders supported by transverse floor beams, forming the primary load transfer mechanism. The general geometric configuration, span arrangement, and structural layout of the bridge are summarized in Table 1. The bridge layout, elevation, and overall structural configuration are illustrated in Figure 1 – Figure 3.

Table 1: Bridge data

Bridge type	Girder and truss bridges
Located	Pasirjengkol – Wanaraja
Bridge length	41.055 m
Bridge width	1.30 m; 3.60 m; 1.30 m
Width between rails	1.20 m
Number of spans	3 spans
Span configuration	9.485 m; 21.930 m; 9.635 m
Bottom structure type	Stone masonry

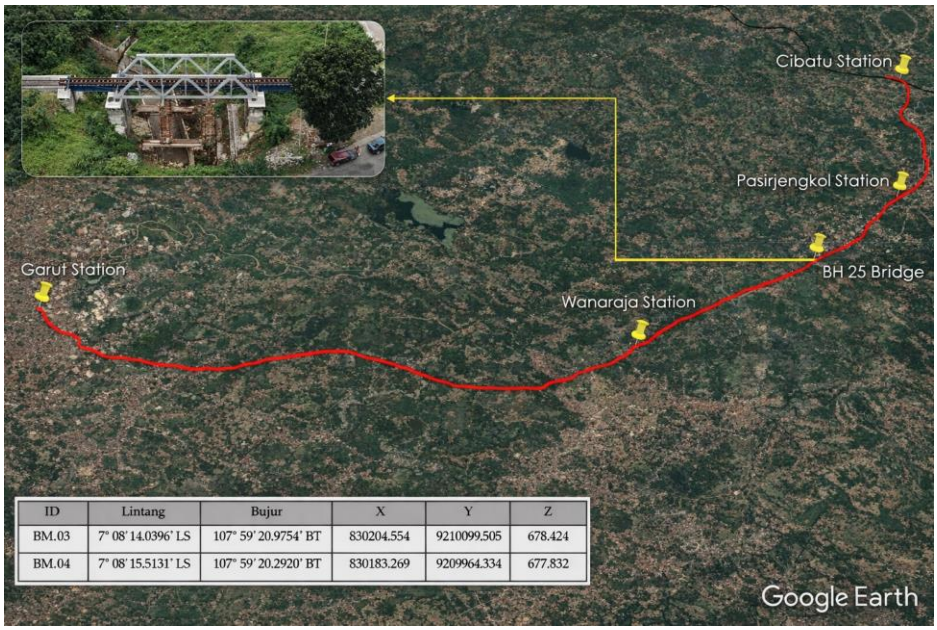

ID	Lintang	Bujur	X	Y	Z
BM.03	7° 08' 14.0396" LS	107° 59' 20.9754" BT	830204.554	9210099.505	678.424
BM.04	7° 08' 15.5131" LS	107° 59' 20.2920" BT	830183.269	9209964.334	677.832

Figure 1: Cibatu - Garut Railway Map

(a) (b)

Figure 2: (a) Aerial view of the bridge, (b) Steel structure of the bridge

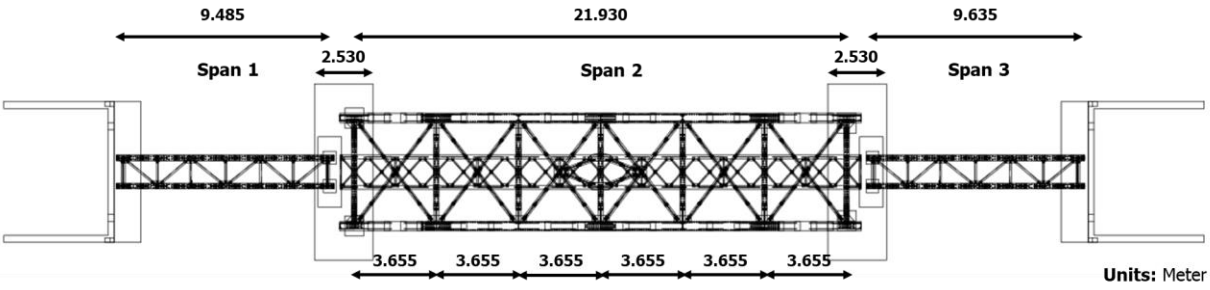

Figure 3: Top view of the bridge

Span 2 was identified as the most critical segment due to observable camber deficiency and the presence of temporary supports. Although the bridge was originally designed with a positive camber to compensate for dead and live load effects, construction deviations resulted in a downward displacement, indicating reduced global stiffness and motivating further structural evaluation.

3.2. Load Testing Program

Static and dynamic load tests were conducted using a CC206 diesel-electric locomotive with a total weight of 90 tons and an axle load of 15 tons. The locomotive specifications, static loading configuration, and governing load combinations applied during the field test are listed in Table 2. The geometric properties and section characteristics of the bridge members, together with the adopted material properties of the existing steel components, are summarized in Table 3, respectively. The loading positions during testing are illustrated in Figure 4 and 5.

Table 2: CC206 Locomotive specifications

Technical data	
Locomotive	CC 206 13 21
Power source	Diesel electric
Model	GE CM20EMP
Wheel specifications	
Whyte notation	0-6-6-0
AAR wheel setup	C-C
UIC classification	Co'Co'
Dimensions	
Track width	1.067 m (3 ft 6 in)
Length	15.849 m (17 yd 1 ft 0 in)
Width	2.743 m (3 yd 0 ft 0 in)
Maximum height	3.695 m (4 yd 0 ft 0 in)
Axle load	15 tons (15 tons length; 17 tons short)
Weight	
Empty weight	88.2 tons (86.8 tons length; 97.2 tons short)
Ready weight	90 tons (89 tons length; 99 tons short)
Performance	
Maximum speed	160 km/h (44 m/s) Original Speed; 120 km/h (33 m/s) Operational Speed
Engine power	1.680 kW (2.250 hp)
Tractive force	248 kN (56.000 lbf)

Table 3: Dimension of bridge structure

No.	Bridge Structure (A)	Span	Profil type	Truss Structure (B)	Profil type
1	Longitudinal girder	S1 & S3	Steel joist 970.250.10.10	Top & bottom chord	2UNP 220.80.10
2	Longitudinal girder	S2	WF 425.170.18.10	Vertical member	2UNP 220.80.10
3	Transverse girder (top)	S1 & S3	2L 75.75.8	Diagonal 1	2UNP 220.80.10
4	Transverse girder (bottom)	S1 & S3	UNP 140.60.10	Diagonal 2	2UNP 200.75.10.10
5	Transverse girder (mid)	S1 & S3	L 75.75.8	Diagonal 3	2UNP 200.65.10.10
6	Bracing (end)	S1 & S3	2L 75.75.8	-	-
7	Bracing (bottom)	S1 & S3	L 75.75.8	-	-
8	Transverse girder	S2	Steel joist 870.220.10.10	-	-
9	Bracing (bottom)	S2	2L 60.60.8	-	-
10	Bracing (top)	S2	L 55.55.8	-	-

Figure 4: CC206 locomotive used in the load testing program

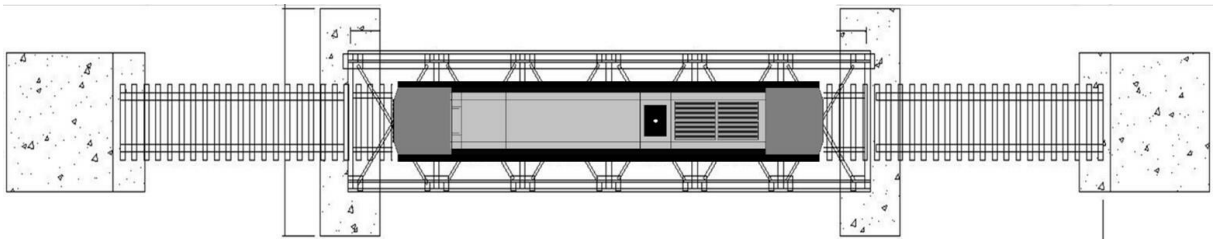

Figure 5: Static load scheme applied to Span 2 of the bridge

Static testing involved positioning the locomotive at predetermined locations along Span 2 to induce maximum deflection and internal forces. Dynamic testing was performed through controlled locomotive passage to capture vibration responses under moving loads, following Indonesian railway safety regulations and international testing guidelines. The evaluation procedures and acceptance criteria were further interpreted with reference to national structural design provisions to ensure consistency with prevailing code-based safety requirements.

3.3. Instrumentation and Measurement System

The structural response of the bridge was monitored using a combination of displacement, strain and acceleration measurement systems. Linear Variable Differential Transformers (LVDTs) and strain gauge were used to measure vertical deflections at critical locations, particularly at the midspan of Span 2 as shown in Figure 6 and 7. The LVDTs had a measurement range of ±50 mm with an accuracy of ±0.01 mm. Dynamic response measurements were obtained using uniaxial accelerometers installed at selected locations along the bridge deck. The acceleration response was measured using accelerometers with a sensitivity of approximately 400 mV/g and an effective frequency range of up to 200 Hz, making them suitable for capturing the dominant vibration modes of railway bridge structures. All sensors were connected to a centralized data acquisition system with a sampling frequency of 200 Hz, ensuring sufficient resolution for both static and dynamic response measurements in accordance with the Nyquist criterion. Signal conditioning modules were employed to filter noise and stabilize the recorded signals, thereby enhancing data quality and reliability for subsequent frequency-domain analysis.

The measurement chain consisted of sensor installation, signal transmission, data acquisition, and post-processing. Sensors were carefully calibrated prior to installation, and their placement was selected to capture both global structural response and localized behaviour. The recorded data were processed using standard signal analysis techniques, including filtering and frequency domain analysis, to extract relevant structural parameters such as deflection and natural frequencies. This instrumentation setup ensures sufficient accuracy and reliability of the measurements, allowing for a robust evaluation of the structural performance under operational loading conditions. The adopted instrumentation and measurement procedure is consistent with commonly accepted practices in full-scale bridge load testing, ensuring the reliability and reproducibility of the results.

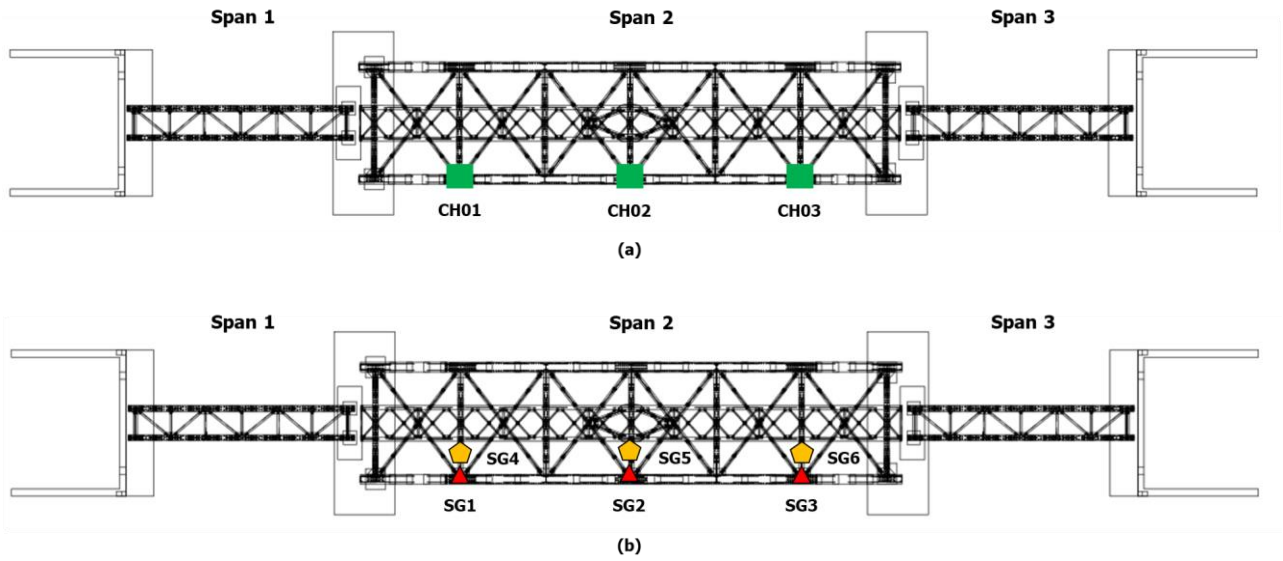

Figure 6: (a) Installation of the LVDT sensor on the bridge superstructure; (b) Installation of the strain gauge sensor on the bridge superstructure

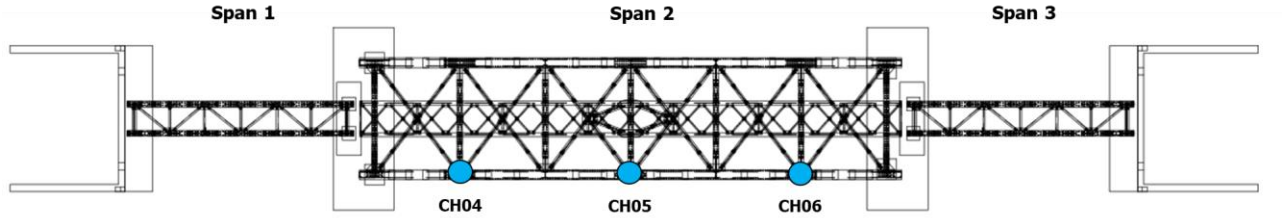

Figure 7: Installation of accelerometer sensors on the bridge structure

Sensors were installed at 1/4L, 1/2L, and 3/4L of Span 2 to capture representative global and local behaviour. This configuration ensured reliable evaluation of serviceability, stiffness, and dynamic characteristics.

3.4. Numerical Modelling and Model Calibration

A three-dimensional finite element model of the BH 25 railway bridge was developed in SAP2000 to simulate its response under static and dynamic loading. The model accurately represents the bridge geometry and structural system, with main truss members idealized as frame elements capturing axial, flexural, and shear behaviour, and the deck and secondary components modelled using equivalent beam elements. All connections were assumed rigid, and boundary conditions were defined to reflect the actual support system. Material properties were assigned based on standard steel parameters, including elastic modulus and mass density. The modelling framework, including geometry, boundary conditions, and mesh discretization, is presented in Figure 8 and 9.

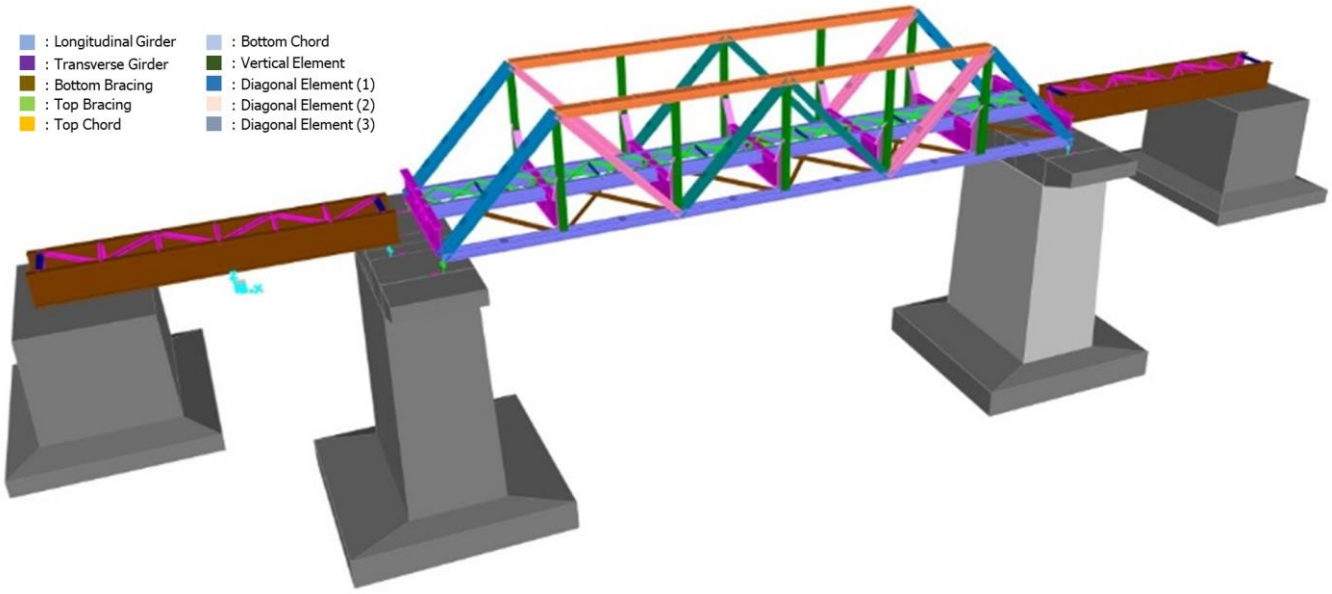

Figure 8: Three-dimensional model of bridge structure

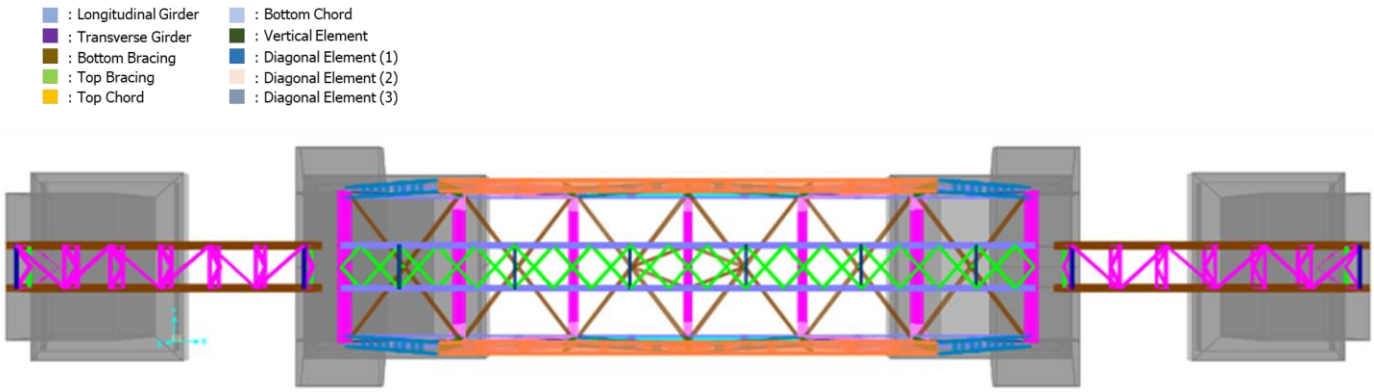

Figure 9: Top view of the bridge structure model

Model calibration was conducted through an iterative adjustment of the effective elastic modulus of steel members and boundary stiffness parameters to achieve agreement between measured and analytical structural responses. Two quantitative indicators were selected as calibration targets: (i) midspan deflection under static loading and (ii) dominant vertical natural frequency obtained from dynamic testing. The relative difference between numerical prediction and field measurement was evaluated as:

$$Difference\ (\%) = \frac{|FEM - Field|}{|Field|}\ x\ 100 \quad (1)$$

Convergence was considered satisfactory when the frequency deviation was below 5% and the deflection deviation remained within acceptable engineering tolerance for conservative capacity evaluation.

4. Results and Discussion

4.1. Static Load Test Result

According to the Regulation of the Minister of Transportation of the Republic of Indonesia No. 69 of 2018, the allowable vertical deflection for railway bridges under service loading is typically limited to L/1000, where L denotes the span length. This limit is widely used as a serviceability criterion to ensure structural performance and operational safety under railway loading conditions.

The maximum measured mid-span deflection at Span 2 under static load was −11.30 mm, which is significantly lower than the allowable limit of L/1000 (21.93 mm). The measured deflection results and the corresponding allowable limits for the tested load cases are presented in Figure 10. A summary of the deflections at 1/4L, 1/2L, and 3/4L is shown in Figure 11.

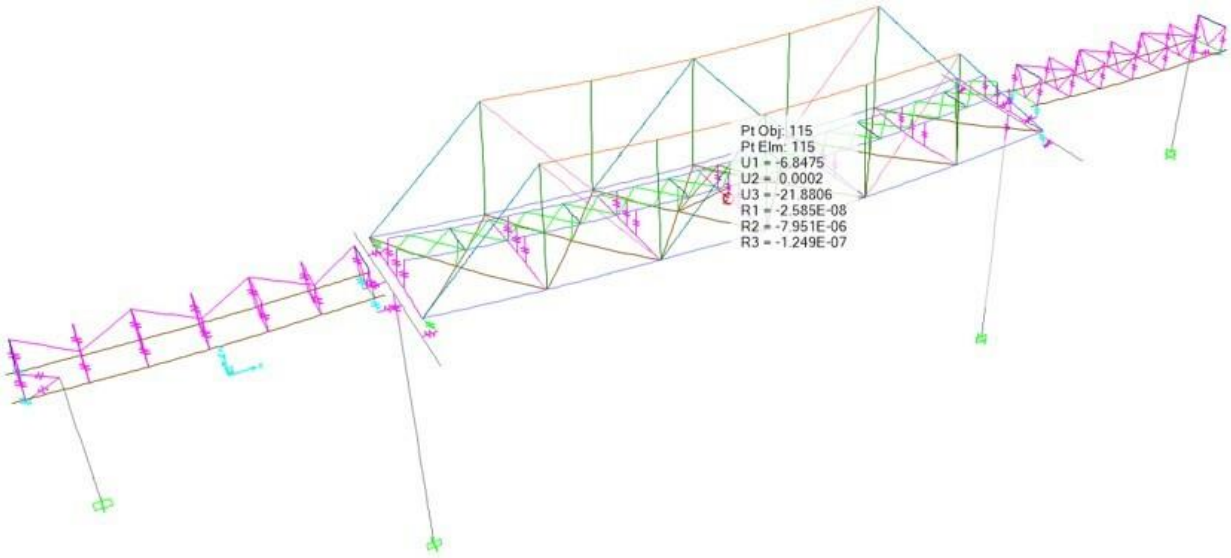

Figure 10: Deflection at midspan (1/2L) of Span 2 under service load: –21.88 mm

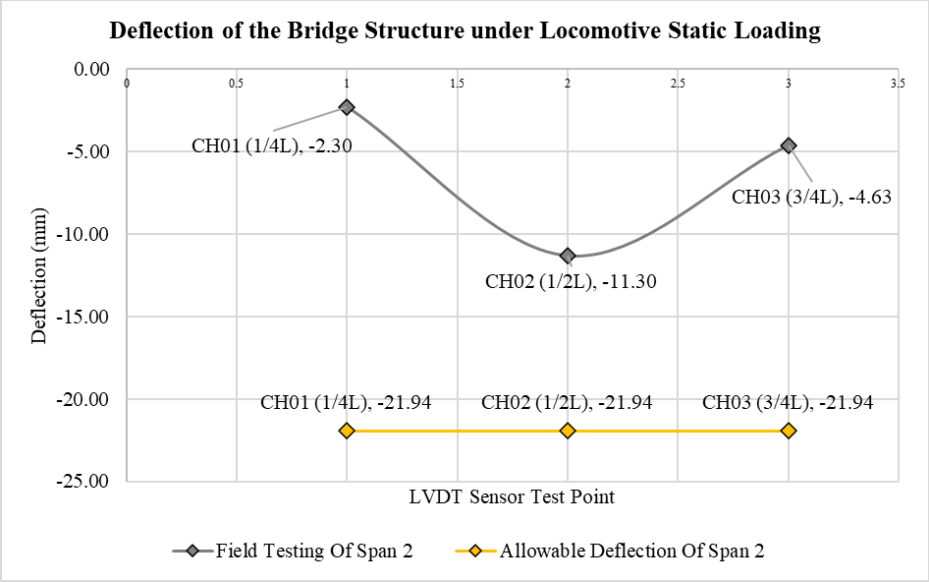

Figure 11: Deflection of the bridge structure under locomotive static loading

It should be noted that two deflection values are discussed in this study. The value of −11.30 mm represents the maximum midspan deflection recorded during full-scale field testing under operational loading. Meanwhile, the value of −21.88 mm corresponds to the analytical prediction obtained from the finite element model under the governing load combination prior to strengthening. The difference between these values reflects the distinction between measured field response and model-based structural analysis.

Table 4: Field vs. FEM comparison

Parameter	Field measurement	FEM prediction	Difference [%]
Midspan deflection [mm]	-11.30	-21.88	48.4%
Dominant frequency [Hz]	14.65	14.98	2.25%

The analytical prediction provides a conservative estimate relative to field measurements, supporting the reliability and safety-oriented applicability of the numerical model for subsequent structural capacity evaluation.

Although the calibrated model reproduced the dominant natural frequency within 2.25%, the predicted static midspan deflection remained larger than the field-measured value, resulting in a relative difference of approximately 48.4%. This deviation reflects a deliberate conservative modelling strategy adopted for capacity-oriented assessment. Rather than enforcing exact deflection matching, calibration prioritized accurate representation of global stiffness through dynamic response agreement, while maintaining conservative displacement predictions to avoid overestimation of structural capacity. Such an approach is considered acceptable in safety-critical infrastructure evaluation, where conservative demand estimation provides a defensible basis for strengthening decisions.

Elongation (ΔL) of the span-2 bridge girder was monitored using strain gauges installed at 1/4L, 1/2L, and 3/4L under static locomotive loading, where positive and negative values denote tension and compression, respectively. The bottom chord exhibited tensile elongation, while the top chord showed compressive elongation; strain was evaluated using $\varepsilon = \Delta L/L$ with a gauge length of 160 mm and subsequently converted to stress. The maximum tensile and compressive stresses were 111 MPa and – 124 MPa, respectively, both significantly lower than the steel yield strength (fy = 349 MPa), indicating adequate structural performance under the applied load.

Table 5: Calculated strain values of the Span-2 bridge girder based on strain gauge measurements

Field testing scheme	Static load [ton]	Testing points	Strain [mm/mm]
Static load B2	90,00	SG1 (1/4L) B2 RB	0.00026
		SG2 (1/2L) B2 RB	0.00019
		SG3 (3/4L) B2 RB	0.00056
		SG4 (1/4L) B2 RA	-0.00062
		SG5 (1/2L) B2 RA	-0.00051
		SG6 (3/4L) B2 RA	-0.00050

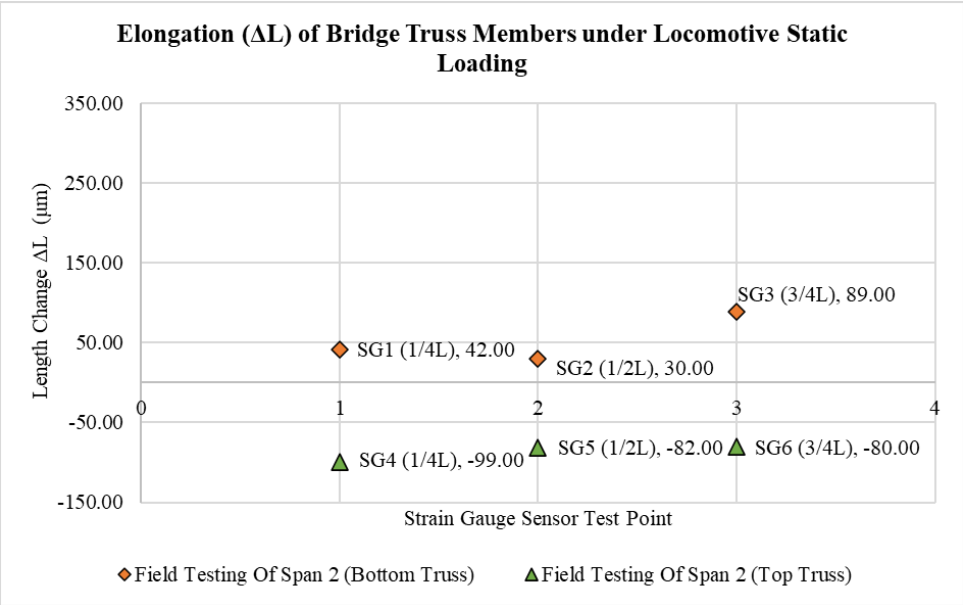

Figure 12: Measured elongation (ΔL) distribution of the Span-2 bridge girder under static locomotive loading

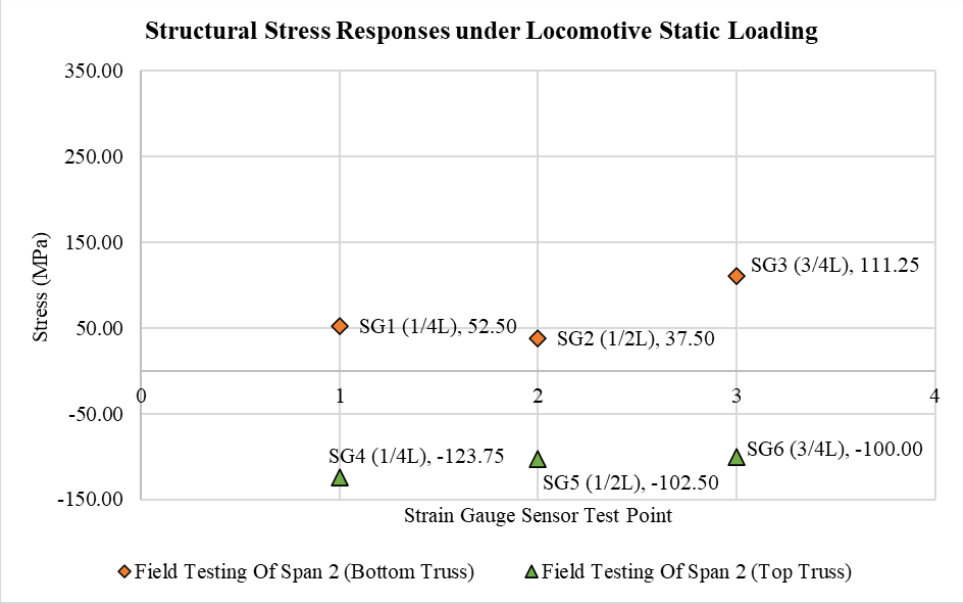

Figure 13: Stress distribution of the Span-2 bridge girder derived from strain gauge measurements

The close agreement between different measurement techniques confirms the reliability of the recorded data and indicates elastic structural behaviour under service loading conditions.

4.2. Dynamic Load Test Result

Frequency-domain analysis was conducted using the Fast Fourier Transform (FFT) to transform time-domain signals into the frequency domain, from which the fundamental frequency was identified as the dominant peak corresponding to the global vibration mode, to ensure reliability, multiple measurements were analysed for consistency, and the resulting dominant vertical natural frequency of 14.65 Hz slightly lower than that predicted by the calibrated finite element model was subsequently compared with analytical results for validation, as illustrated in Figure 14 and 15.

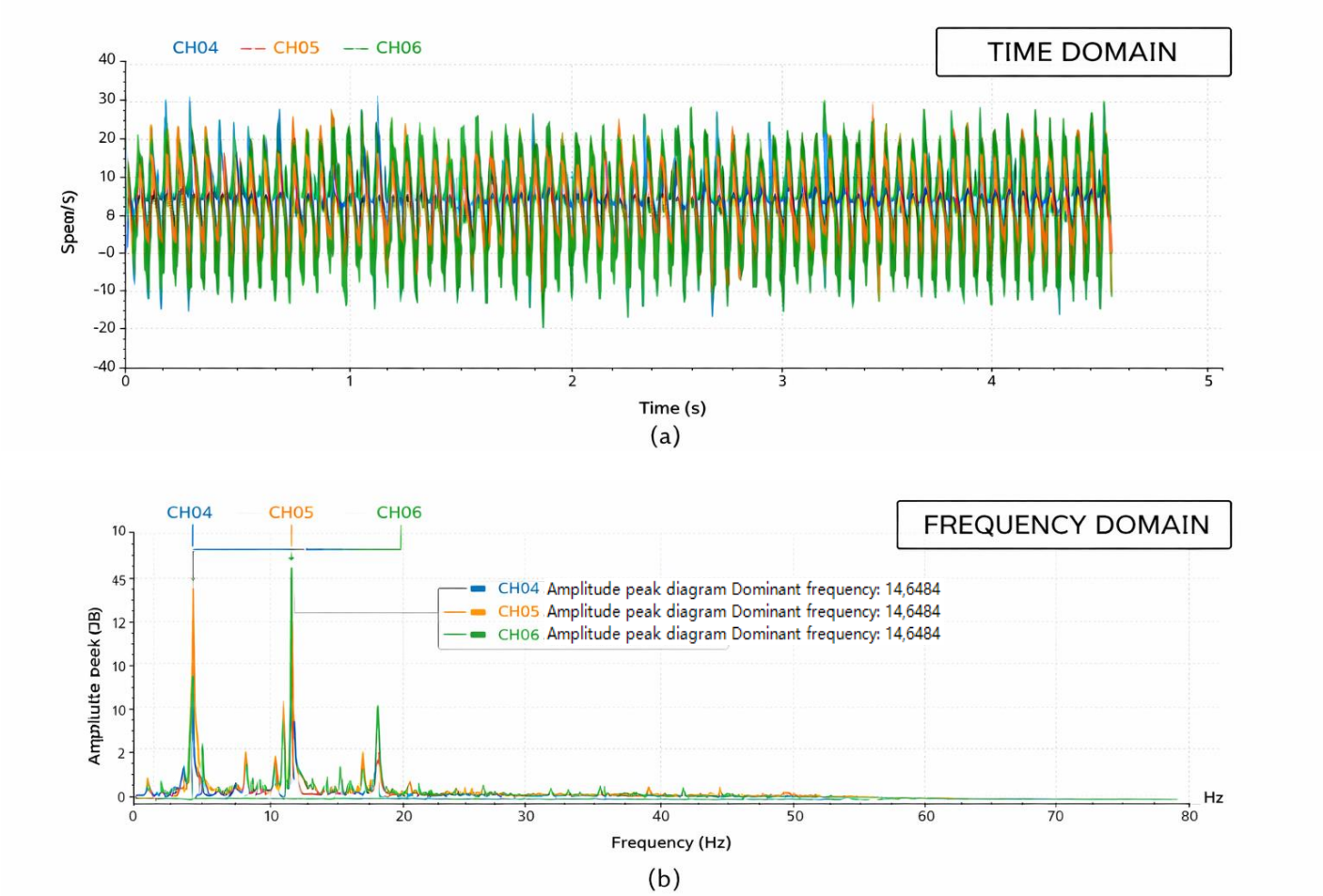

Figure 14: Dominant vertical (z-Direction) frequency of the bridge girders: (a) Time-domain response; (b) Frequency-domain response

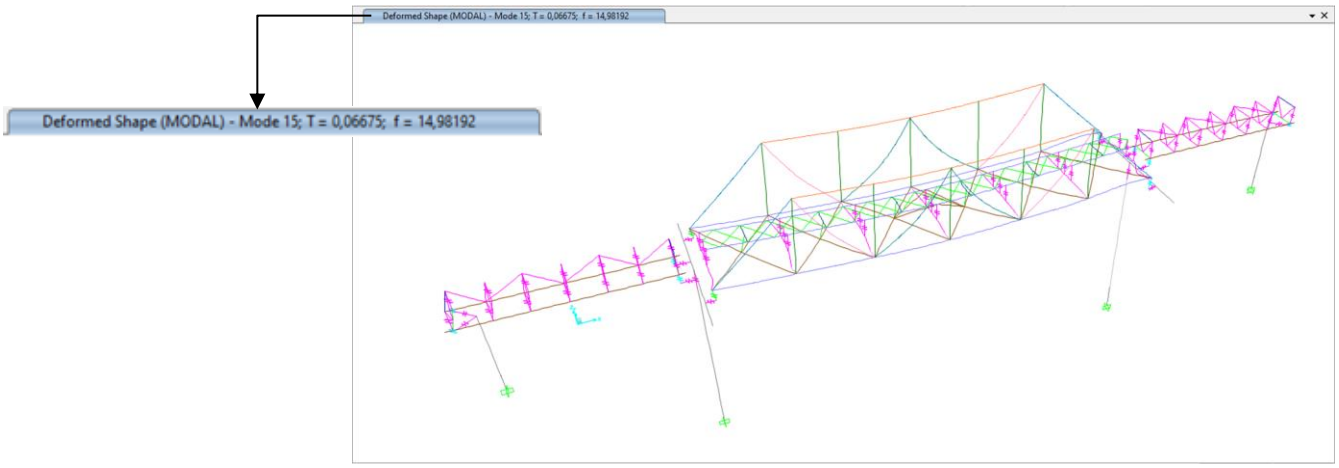

Figure 15: Dominant vertical mode (Mode 15) of the bridge structure with a frequency of 14.98 Hz

The increase in dominant natural frequency after strengthening reflects a measurable enhancement in global structural stiffness, consistent with the theoretical relationship between stiffness and natural frequency ($f = \sqrt{k/m}$). This confirms that the strengthening intervention not only improved member-level capacity but also restored system-level structural rigidity.

4.3. Structural Capacity Evaluation

Although the bridge meets the serviceability requirements under static loads, the structural capacity evaluation indicates that strength-related deficiencies still exist in some critical elements of Span 2, indicating that acceptable deflection performance does not necessarily imply adequate structural safety. The calculated internal forces of the critical elements under the principal load cases provide quantitative evidence of this condition, as reflected by the demand-to-capacity ratios exceeding unity observed in some truss elements under the principal load combinations (Table 6). The overall distribution of member capacity ratios prior to strengthening further illustrates the extent of strength deficiency within the truss system (Figure 16).

Table 6: Demand-to-capacity ratios of structural elements in Span 2 under governing load combinations

No.	Structural elements	Profil type	Capacity ratio	Allowable capacity ratio	Description
1	Longitudinal girder	WF 425.170.18.10	0.597	1.0	OK
2	Transverse girder	870.220.10.10	1.683	1.0	Not OK
3	Bottom bracing	2L 60.60.8	1.045	1.0	Not OK
4	Top bracing	L 55.55.8	0.579	1.0	OK
5	Top chord	2UNP 220.80.10	0.697	1.0	OK
6	Bottom chord	2UNP 220.80.10	2.856	1.0	Not OK
7	Vertical element	2UNP 220.80.10	0.620	1.0	OK
8	Diagonal element 1	2UNP 220.80.10.10	0.571	1.0	OK
9	Diagonal element 2	2UNP 220.75.10.10	0.476	1.0	OK
10	Diagonal element 3	2UNP 220.65.10.10	0.122	1.0	OK

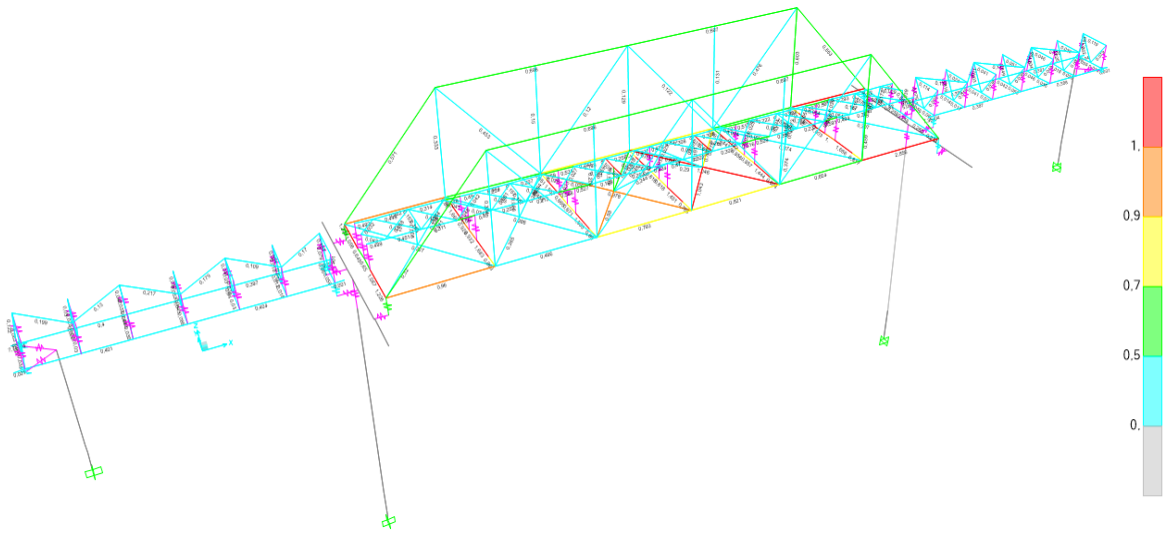

Figure 16: Capacity ratios of the bridge structure elements

It is important to note that serviceability compliance prior to strengthening did not guarantee adequate structural safety, as several members exhibited demand-to-capacity ratios exceeding unity. This finding underscores a fundamental limitation of deflection-based assessment approaches when applied to aging truss systems, where localized overstress may remain undetected despite acceptable global displacement behaviour. The integrated workflow adopted in this study demonstrates that stiffness indicators alone are insufficient without concurrent capacity verification, particularly for bridges subjected to long-term deterioration and cumulative fatigue effects.

4.4. Strengthening by External Prestressing

To address the identified strength deficiencies, an external prestressing system was implemented in combination with local steel plate reinforcement. The adopted strengthening configuration, tendon profile, and anchorage system are illustrated in Figure 18 and 19. The introduction of prestressing forces modified the internal force distribution within the truss members, resulting in a systematic reduction in member utilization levels and an overall improvement in structural capacity.

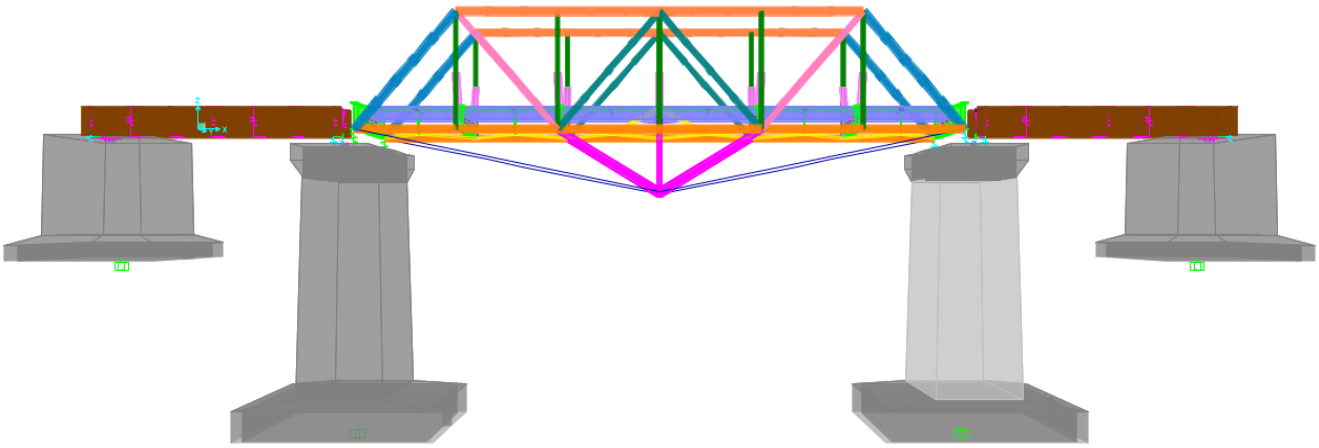

Figure 17: Side view of the external prestressing reinforcement model of the bridge structure

Table 7: Modelling criteria for bridge structure reinforcement

Tendon diameter	43.575 mm
Tendon area	1491.334 mm^2
Strand type	7-wire strand
Dimensions of deviator profile	H 200.200.8.12
Prestressing force	1942 kN

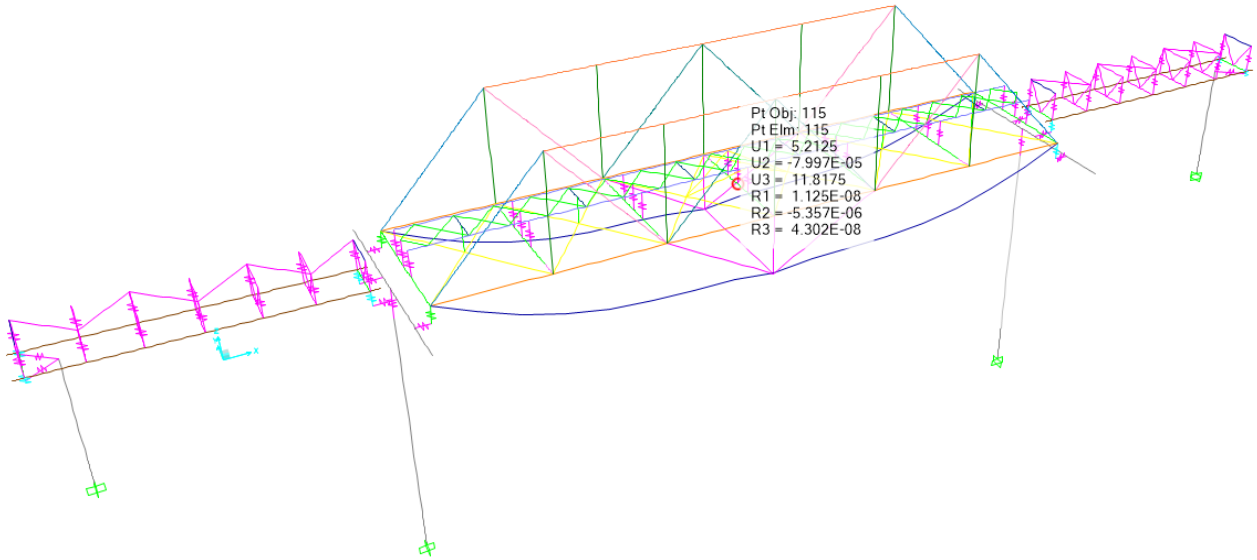

Figure 18: Midspan (1/2L) deflection of the bridge structure after external prestressing under the load combination 1.0D + 1.0SD + 1.0PR

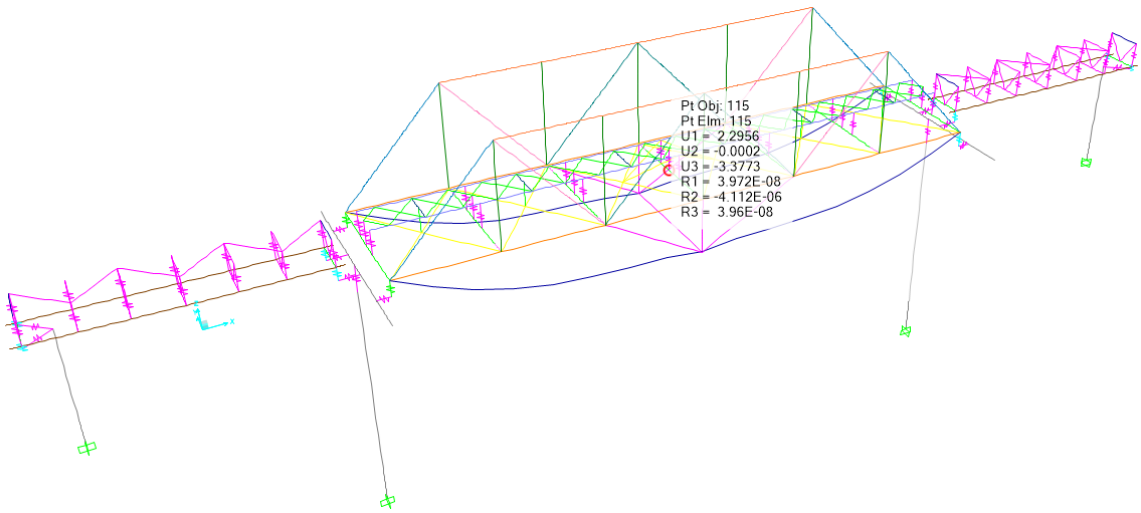

Figure 19: Midspan (1/2L) deflection of the bridge structure after external prestressing under the load combination 1.0D + 1.0SD + 1.0LL + 1.0PR

The effectiveness of the strengthening intervention is evidenced by the post-strengthening capacity evaluation, which demonstrates a consistent decrease in demand-to-capacity ratios across critical members (Table 9). In addition to strength enhancement, the strengthening scheme also led to an improvement in global stiffness, as indicated by the increase in the dominant natural frequency to 17.07 Hz (Figure 20). Local plate reinforcement further contributed to reducing all member capacity ratios to acceptable limits, as confirmed by the final capacity assessment results (Table 9 and Figure 21).

Table 8: Comparison of midspan deflections before and after external prestressing

Description	Load combination	Deflection structure [mm]
		1/2L
Field testing	1.0 D + 1.0 SD + 1.0 LL	-11.30
External prestressing reinforcement	1.0 D + 1.0 SD + 1.0 PR	11.82
	1.0 D + 1.0 SD + 1.0 LL + 1.0 PR	-3.38

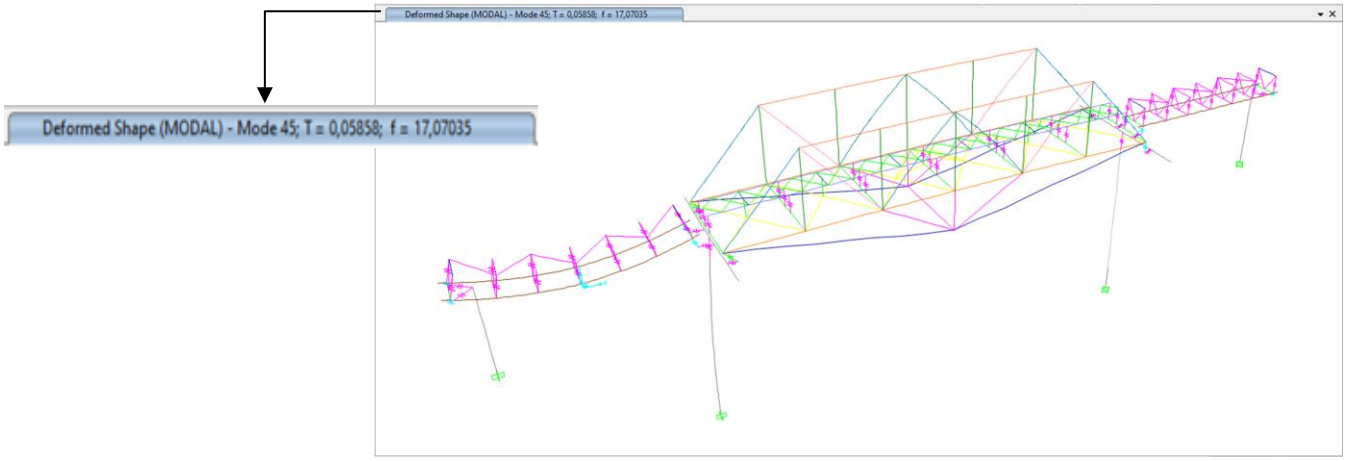

Figure 20: Dominant vertical (z-Direction) vibration mode (Mode 45) of the bridge structure after external prestressing and plate reinforcement, with a frequency of 17.07 Hz

Table 9: Capacity ratios of bridge elements after external prestressing and plate reinforcement

No.	Structural elements	Profil type	Capacity ratio	Allowable capacity ratio	Description
1	Longitudinal girder	WF 425.170.18.10	0.570	1.0	OK
2	Transverse girder	870.220.10.10	0.975	1.0	OK
3	Bottom bracing	2L 60.60.8	0.677	1.0	OK
4	Top Bracing	L 55.55.8	0.291	1.0	OK
5	Top chord	2UNP 220.80.10	0.334	1.0	OK
6	Bottom chord	2UNP 220.80.10	0.949	1.0	OK
7	Vertical element	2UNP 220.80.10	0.235	1.0	OK
8	Diagonal element 1	2UNP 220.80.10.10	0.332	1.0	OK
9	Diagonal element 2	2UNP 220.75.10.10	0.322	1.0	OK
10	Diagonal element 3	2UNP 220.65.10.10	0.044	1.0	OK
11	Deviator	H 200.200.8.12	0.542	1.0	OK

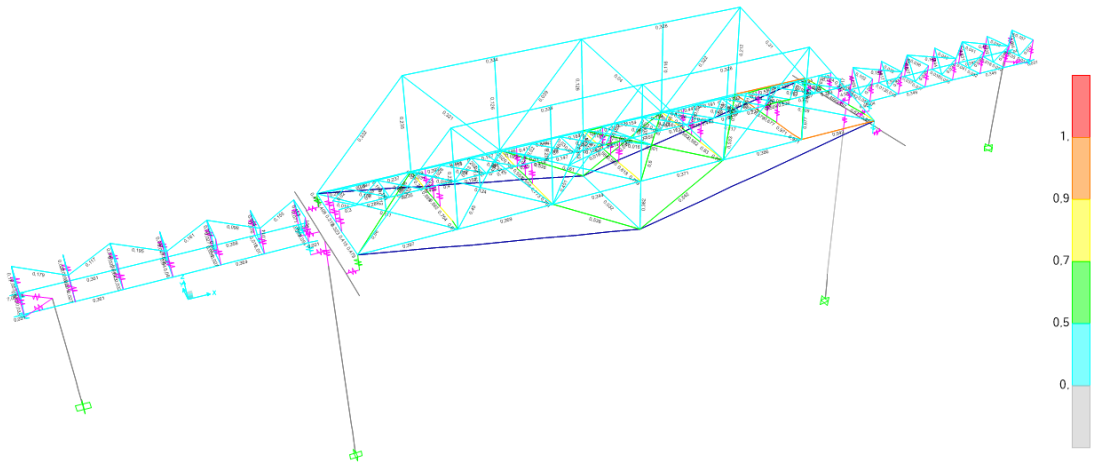

Figure 21: Capacity ratios of bridge elements after external prestressing and plate reinforcement

These results confirm that externally prestressed strengthening, when properly integrated with localized reinforcement, constitutes an effective and rational strategy for restoring both stiffness and load-carrying capacity in aging steel railway bridges. Unlike previous studies that predominantly report analytical or laboratory-scale validations, the present study provides rare full-scale field evidence from an operational bridge. The observed increase in dominant natural frequency from 14.65 Hz to 17.07 Hz corresponding to a 16.5% increase demonstrates measurable global stiffness recovery. This level of enhancement indicates substantial stiffness improvement and aligns with stiffness recovery trends reported in recent strengthening and railway bridge assessment studies.

5. Conclusion

The BH 25 railway bridge satisfies serviceability requirements under operational loading but exhibits reduced global stiffness and localized capacity deficiencies due to aging and construction deviations. The integrated use of static and dynamic load testing, calibrated numerical modelling, and capacity evaluation provides a comprehensive assessment of the bridge's structural condition.

Theoretically, the findings highlight the importance of combining static and dynamic indicators to capture stiffness degradation mechanisms. Practically, the results demonstrate that external prestressing, complemented by local reinforcement, offers an effective and minimally invasive solution for extending the service life of aging railway bridges.

Future research should focus on long-term monitoring of strengthened bridges to evaluate time-dependent behaviour, fatigue performance, and durability under repeated railway loading, as well as on applying the proposed

framework to other bridge typologies. In particular, long-term monitoring is required to evaluate prestress loss, fatigue performance of strengthened members, and durability under repeated railway loading.

Beyond the specific case study, this research demonstrates a replicable integrated assessment methodology that links field-measured stiffness indicators to quantified structural capacity evaluation and strengthening verification. The framework contributes to reducing uncertainty in performance-based bridge management and provides a structured basis for decision-making in aging railway infrastructure systems.

Theoretical Implications

From a theoretical perspective, the results highlight the importance of combining static and dynamic indicators to capture stiffness degradation mechanisms that cannot be identified through serviceability-based evaluation alone. The integration of field measurements with calibrated numerical modelling improves the reliability of structural diagnosis for aging steel railway bridges.

Practical Implications

From a practical engineering perspective, the findings demonstrate that external prestressing, when properly integrated with local reinforcement, provides an effective and minimally invasive strengthening strategy for extending the service life of existing railway bridges under operational loading conditions.

Limitations and Applicability

While the proposed framework is demonstrated on a single steel truss railway bridge, the methodology is applicable to other existing railway bridges with similar structural typologies and loading characteristics. Nevertheless, the effectiveness of external prestressing may vary depending on bridge configuration, boundary conditions, and deterioration mechanisms. Therefore, future applications should be supported by bridge-specific assessment and model calibration.

Statement and Declarations

Author Contributions: Sumargo led the conceptualization and drafting of the manuscript and contributed to the methodology, formal analysis, and review; Mardiana Oesman contributed to the methodology, formal analysis, review, and supervision; Fachmi Fadli conducted the investigation and data curation. All authors approved the final manuscript.

Conflict of Interest Statement

The authors declare that there is no conflict of interest regarding the publication of this paper.

Data Availability Statement

The data used to support the findings of this study are available from the corresponding author upon reasonable request.

Funding Statement

The authors declare that no funds, grants, or other financial support were received for the preparation of this study.

AI Usage Statement

During the preparation of this manuscript, the authors used artificial intelligence tools (including ChatGPT, OpenAI) solely for language refinement, paraphrasing, and formatting assistance to improve clarity and readability. These tools were

not used for data analysis, interpretation of results, methodological development, or the generation of scientific content. All outputs generated by AI tools were carefully reviewed, revised, and validated by the authors, who take full responsibility for the accuracy, integrity, and content of the published article.

References

Armijo, A., et al. (2024). Integration of railway bridge structural health monitoring and digital twin using low-cost wireless accelerometers and machine learning. Sensors, 24(7), 2115. https://doi.org/10.3390/s24072115.

Atta, A. M., et al. (2024). Effectiveness of external prestressing in enhancing the non-ductile hanger failure mitigation of inverted T-beams. Frontiers of Structural and Civil Engineering. https://doi.org/10.1007/s11709-024-1026-x.

Bacinskas, D., Kamaitis, Z., Jatulis, D., & Kilikevicius, A. (2013). Load testing and model updating of a single-span composite steel–concrete railway bridge. Procedia Engineering, 57, 127–135. https://doi.org/10.1016/j.proeng.2013.04.019.

Bayraktar, A., et al. (2017). Static and dynamic field load testing of the long span Nissibi cable-stayed bridge. Soil Dynamics and Earthquake Engineering, 94, pp. 136-157. https://doi.org/10.1016/j.soildyn.2017.01.019.

Bertolesi, E., Buitrago, M., Adam, J. M., & Calderón, P. A. (2021). Fatigue assessment of steel riveted railway bridges: Full-scale tests and analytical approach. Journal of Constructional Steel Research, 182, 106664. https://doi.org/10.1016/j.jcsr.2021.106664.

Bień, J., Kużawa, M., & Kamiński, T. (2020). Strategies and tools for the monitoring of concrete bridges. Structural Concrete, 21(4), 1227–1239. https://doi.org/10.1002/suco.201900410.

Borzovič, V., Halvonik, J., & Paulík, P. (2026). Experience in monitoring the state of the load-bearing structure of prestressed concrete bridge to extend its operation. Civil and Environmental Engineering, Advance online publication. Sciendo (De Gruyter). https://doi.org/10.2478/cee-2026-0036.

Cao, J., & An, L. (2023). Static load test detection of continuous rigid frame railway bridge. Journal of Architectural Research and Development, 7(5), 1–7. https://doi.org/10.26689/jard.v7i5.5207.

Chacón, R., et al. (2024). Digital twinning during load tests of railway bridges: Case study of the high-speed railway network, Extremadura, Spain. Structure and Infrastructure Engineering, 20(7–8), 1105–1119. https://doi.org/10.1080/15732479.2023.2264840.

Duvnjak, I., Bartolac, M., Damjanović, D., & Košćak, J. (2020). Performance assessment of a concrete railway bridge by diagnostic load testing. Structural Concrete, 21(6), 2363–2376. https://doi.org/10.1002/suco.201900491.

Duvnjak, I., Damjanović, D., Bartolac, M., Frančić Smrkić, M., & Skender, A. (2019). Monitoring and diagnostic load testing of a damaged railway bridge. Frontiers in Built Environment, 5, 108. https://doi.org/10.3389/fbuil.2019.00108.

Fang, D., et al. (2024). Flexural performance and stress calculation of external prestressing using FRP bars. Materials, 17(5), 1130. https://doi.org/10.3390/ma17051130.

Fawad, M., et al. (2023). Automation of structural health monitoring (SHM) system of a bridge using BIMification approach. Scientific Reports. https://doi.org/10.1038/s41598-023-40355-7.

Gedam, V. G., Meshram, V., & Mase, D. (2020). Condition assessment and structural analysis of P.C.C railway bridge. International Research Journal of Engineering and Technology, 7(11), 1199–1205.

Guo, H., et al. (2024). Monitoring and analysis of prestress loss in prestressed box girder bridges strengthened with external prestressing. Sensors, 24(14), 4549. https://doi.org/10.3390/s24144549.

He, H., et al. (2023). Bridge model updating based on wavelet neural network and wind-driven optimization algorithm. Sensors, 23(22), 9185. https://doi.org/10.3390/s23229185.

Hekič, D., et al. (2024). Improved finite element model updating of a highway viaduct using strain- and acceleration-based analyses. Sensors, 24(9), 2788. https://doi.org/10.3390/s24092788.

Hekič, D., et al. (2025). Model updating of bridges using measured influence lines. Applied Sciences, 15(8), 4514. https://doi.org/10.3390/app15084514.

Hlinka, R., Farbák, M., & Odrobiňák, J. (2024). The use of up-to-date analyses for the temporary bridges application in the present. Civil and Environmental Engineering, 20(1), 491–507. Sciendo (De Gruyter). https://doi.org/10.2478/cee-2024-0038.

Innocenzi, R. D., et al. (2022). A Good Practice for the Proof Testing of Cable-Stayed Bridges. Applied Science. 2022, 12, 3547. https://doi.org/10.3390/app12073547.

Karavasilis, T. L., Lou, T., & Chen, B. (2021). Assessment of second-order effect in externally prestressed steel–concrete composite beams. Journal of Bridge Engineering, 26(6). https://doi.org/10.1061/(ASCE)BE.1943-5592.0001718.

Kim, S. W., Yun, D. W., Chang, S. J., Park, D. U., & Park, J. B. (2022). Dynamic stability assessment of high-speed railway bridges using numerical model updating. Applied Sciences, 12(8), 3948. https://doi.org/10.3390/app12083948.

Minister of Transportation of the Republic of Indonesia. (2018). Regulation of the Minister of Transportation of the Republic of Indonesia. No 69 of 2018. Railway safety management systems.

Li, L., & Ohkubo, T. (2024). Wireless vibration testing and bridge deck damage identification using underneath maintenance walkway. Scientific Reports. https://doi.org/10.1038/s41598-024-77179-y.

Liu, Z., et al. (2024). Load testing and analysis of a large span through simply-supported steel box arch bridge. Applied Sciences, 14(23), 11418. https://doi.org/10.3390/app142311418.

Lantsoght, E. O. L., Schmidt, J. W., & Sas, G. (2024). Bridge load testing: Recent advances in research, collaboration, and codes. https://doi.org/10.1201/9781003483755-31.

Moravvej, M., et al. (2024). Reference-free vibration-based damage identification of bridges using time–frequency features. Sensors, 24(3), 876. https://doi.org/10.3390/s24030876.

Nawy, E. G. (2009). Prestressed concrete: A fundamental approach. Pearson.

Nhung, N. T. C., et al. (2023). Development and application of LVDT sensors for structural health monitoring of an urban railway bridge in Vietnam. Engineering, Technology & Applied Science Research, 13(5), 11622–11627. https://doi.org/10.48084/etasr.6192.

Odrobiňák, J., Vičan, J., Hlinka, R., Prokop, J., & Vavák, B. (2025). On the load-carrying capacity determination of railway box-girder bridges using the reduced stress method. Civil and Environmental Engineering, Advance online publication. Sciendo (De Gruyter). https://doi.org/10.2478/cee-2026-0021.

Qiao, L., et al. (2025). Analysis of bridge dynamic load test based on millimeter-wave radar. Scientific Reports. https://doi.org/10.1038/s41598-025-96196-z.

Qi, Z., Fang, S., Lin, G., & Wang, H. (2011). Static and dynamic experiment of the behavior of the constructed Hanjiang super-major railway bridge in Laohekou. Advanced Materials Research, 255–260, 1230–1235. https://doi.org/10.4028/www.scientific.net/AMR.255-260.1230.

Rahman, A. K., et al. (2024). A simplified method for estimating bridge frequency effects as a function of train-to-bridge mass ratio. Frontiers in Built Environment. https://doi.org/10.3389/fbuil.2024.1382210.

Recupero, A., Spinella, N., Colajanni, P., & Scilipoti, C. D. (2014). Increasing the capacity of existing bridges by using unbonded prestressing technology: A case study. Advances in Civil Engineering, 2014, 840902. https://doi.org/10.1155/2014/840902.

Rehacek, S., Citek, D., Holy, M., Krystov, M., Citek, A., & Mezera, A. (2026). Diagnostic survey of prestressed concrete bridges in Prague. Civil and Environmental Engineering, Advance online publication. Sciendo (De Gruyter). https://doi.org/10.2478/cee-2026-0049.

Ren, Z., et al. (2025). Bending test and numerical simulation of externally prestressed reinforcement applied to concrete beams. Materials, 18(13), 3024. https://doi.org/10.3390/ma18133024.

Su, H. C., et al. (2024). Fiber monitoring system applied to railway bridge corrosion and deformation assessment. Applied Sciences, 14(17), 7883. https://doi.org/10.3390/app14177883.

Topurova, I. (2023). Testing of a temporary railway bridge and analysis of the results. IOP Conference Series: Materials Science and Engineering, 1297(1), 012003. https://doi.org/10.1088/1757-899x/1297/1/012003.

Zapata, J., et al. (2025). Models for the analysis of the structural capacity of main steel railway bridges. Modeling, 5(2), 38. https://doi.org/10.3390/modeling5020038.

Zhao, H., et al. (2025). Experimental investigation on flexural behavior of precast segmental bridges with external prestressing tendons. Buildings, 15(4), 642. https://doi.org/10.3390/buildings15040642.

Zhou, W., et al. (2025). Finite element model updating for a continuous beam–arch composite bridge based on the RSM and a nutcracker optimization algorithm. Sensors, 25(15), 4831. https://doi.org/10.3390/s25154831.

Zou, Y., et al. (2024). Dynamic response analysis of a train–track–bridge coupled system for railway bridge vibration under train loads. Frontiers in Built Environment. https://doi.org/10.3389/fbuil.2024.1498790.

How to Cite This Article

Sumargo, S., Oesman, M., & Fadli, F. (2026). Integrated Static–dynamic Assessment and Field-validated External Prestressing Strengthening of an Aging Steel Railway Bridge. Civil and Environmental Engineering, 0 (0). https://doi.org/10.2478/cee-2026-0111